

STUDY OF A HIGH-VELOCITY SEPARATOR ON AN ANALOGUE FLUID SYSTEM

E. DUEYMES

Electricité de France, Direction des Etudes et Recherches, Département Machines, 6, quai Watier,
78400 Chatou, France

(Received 15 September 1991; in revised form 5 September 1992)

Abstract—To be able to better control the separation efficiency of a centrifugal-type separator, the high-velocity separator (HVS), a test has been carried out on an analogue fluid system. The actual separator operates at a pressure of some 2 MPa and processes the water/steam system in thermodynamic equilibrium. A mockup on a geometric scale of 0.45 has been tested with a water/argon system at a pressure of 740 kPa and a temperature of approx. 25°C.

Key Words: separation, centrifugal separator, analogue fluid system, small-scale model

1. INTRODUCTION

The tested high-velocity separator (HVS) is of the centrifugal type. It was designed by the Direction des Etudes et Recherches of Electricité de France (EDF) and then developed in collaboration with STEIN-INDUSTRIE.

This piece of equipment is primarily aimed at separating a water/steam mixture at the exhaust of the high-pressure (HP) cylinder of the turbines in PWR nuclear power plants, i.e. at a pressure of around 1 MPa.

After promising results had been obtained in test facilities, two commercial prototypes were constructed and installed in unit 2 of the Bugey power plant near Lyon. Figure 1 shows one of these prototypes.

The two prototypes have been operating since August 1980; their performance characteristics (pressure drops and separation efficiency) come up to our expectations and their mechanical resistance is quite satisfactory. The main test results were described, among others, by Cerdan & Talleu (1984).

Given the excellent operating record of these separators, other applications were contemplated.

Among them, the drying† of the HP steam extracted from the turbines used in PWR power plants is relatively close to the initial application since the fluid system processed is the same. Besides, this application could be easily contemplated as a new generation of HVS had just been developed, the HP recirculation-type HVSs. Indeed, in these separators (see figure 2), the steam extracted in the separation lips together with the separated water to increase separation efficiency is not sent into another external component (a heater in the BUGEY plant) but is sucked along by the hydro-ejector effect and is re-used in the HVS itself. It is not within the scope of this paper to describe the design of these recirculation HVSs in detail. The reader may refer to the descriptions made by Cerdan & Talleu (1984) or Dueymes & Peyrelongue (1990). Nevertheless, a brief description of the principle of operation of this type of HVSs can be given as follows.

Steam laden with water droplets enters the separator (see 10 in figure 4). A swirling motion is imparted to it by a series of fixed turning vanes. The water, of much higher density than the steam, forms a film that runs down the wall (figure 4). The film of water is extracted from the separation cell through an annular skimmer slot (see 7 in figure 4 or 6). The helicoid motion of the main steam

†Drying this steam is one of the means available to protect the HP feedwater heaters against erosion–corrosion phenomena in these power plants.

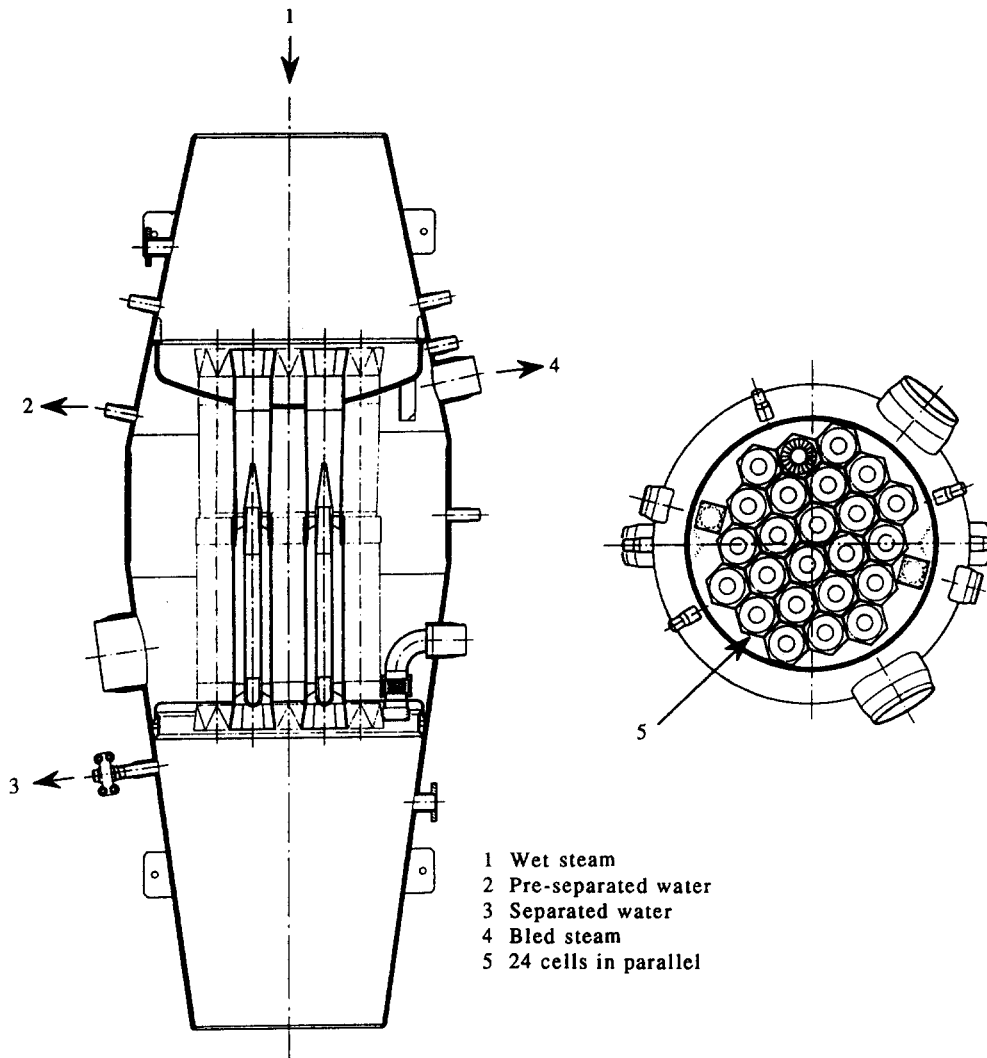


Figure 1. BUGEY prototype.

flow is counteracted by a second series of blades and virtually dry steam leaves the separator (see 4 in figure 4). A small gaseous flow is extracted through the annular skimmer slot, combined with the evacuation of the separated water. The mixture of separated water and extracted steam—called recirculating steam—after passing through the annular skimmer slot, enters the separator's drain collection tank (see 7 and 8 in figure 4). The water flows by gravity to an evacuation nozzle (see 5 in figure 4), while the gas enters the central tube of the HVS cell through a piece in the shape of a water droplet (see 3 or 6 in figure 4). It is then sucked along with the main flow by the hydro-ejector effect thanks to holes (see 1 in figure 4) drilled in the central tube. The path of the recirculating steam is represented in the scheme in figure 2.

Following the first tests on water/steam systems which yielded quite convincing results, EDF decided in 1983 to equip all the HP extraction lines in CP2 900 and 1300 MW PWR units with recirculation HVSs. 100 such separators, each with 4 or 5 HVS cells in parallel, were thus constructed and installed. Figure 3 shows a separator placed on the HP extraction line pipe in a CP2 900 MW PWR unit. Table 1 gives the main operating characteristics.

Note, however, that given the capabilities of EDF's steam/water test rig in Gennevilliers, the recirculation HVS cells could not be preliminarily tested under actual operating conditions (the tests were carried out at pressures below 1.5 MPa instead of the 2–3 MPa corresponding to the actual operating conditions).

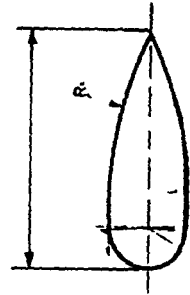
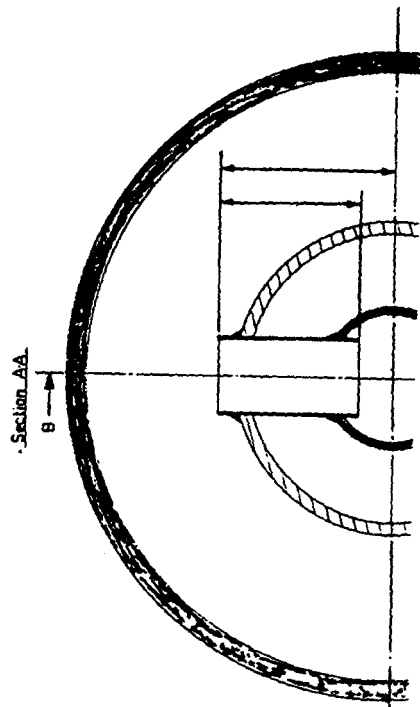
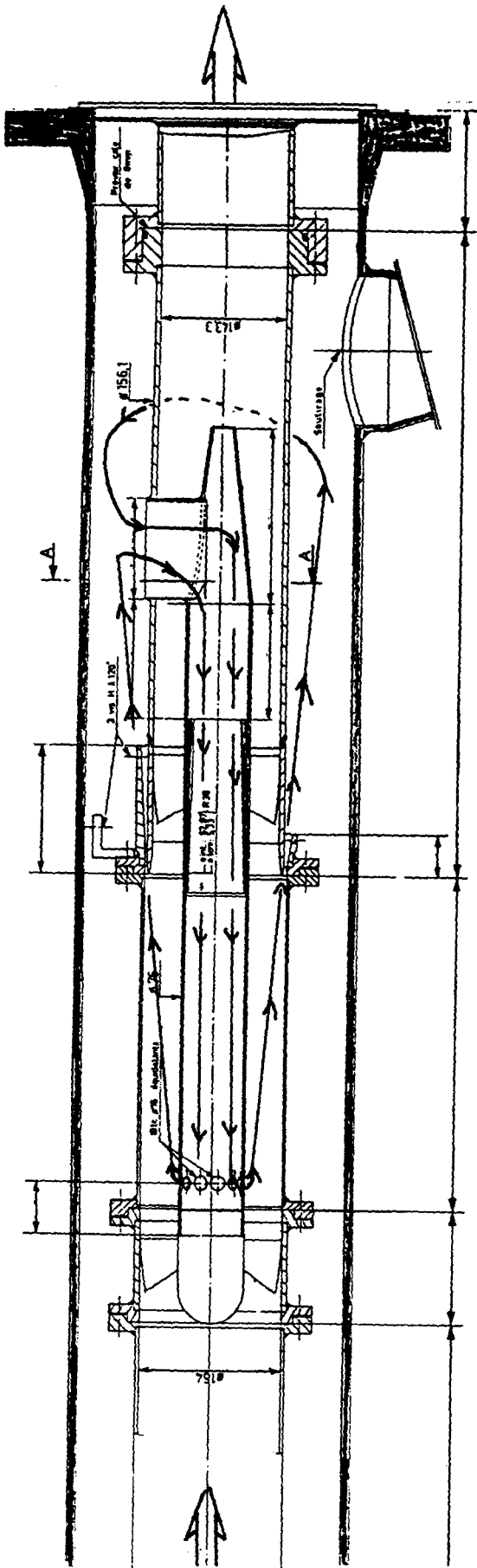


Figure 2. HP recirculation-type HVS.

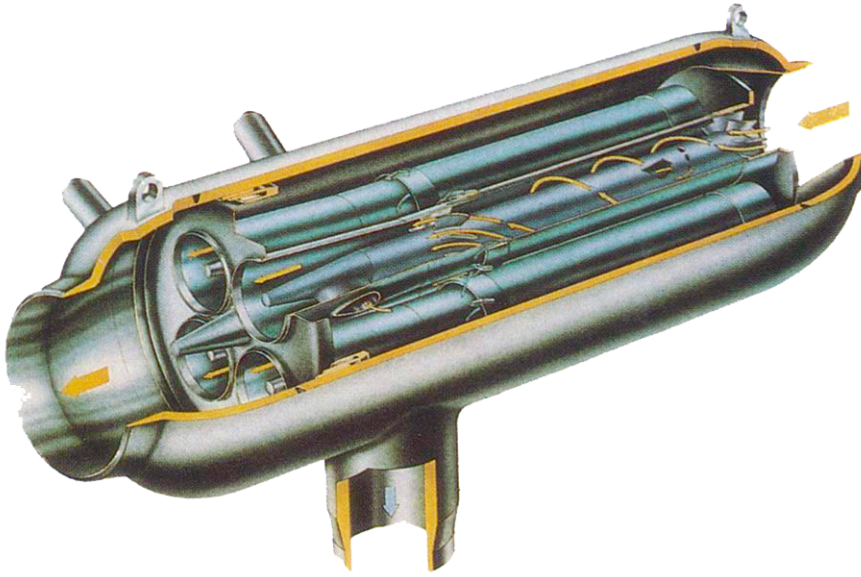


Figure 3. Equipment for an HP extraction line (PWR 900 MW CP2 plant). Diameter = 600 mm, length = 1800 mm, mass = 1000 kg.

2. ON-SITE BEHAVIOUR OF RECIRCULATION HVSs

An on-site control of the separation efficiency of the first separators of this kind was planned. The first control was carried out in October 1984. The methodology adopted consisted of measuring water flowrates with a chemical tracer. It is described for instance by Dueymes (1989a). The separation efficiency measuring procedure itself is depicted by Dueymes (1989b). It already appeared then that the performance characteristics of the separators were appreciably below the values expected as a result of the preliminary tests.

The analysis of the first test results shows that this lower performance cannot be ascribed to a serious error in the design of the separators. Therefore, a number of theoretical as well as experimental studies were undertaken to account for the lower performance characteristics recorded on site. As a result of these studies, the majority of the assumed explanations were eliminated (invalidity of the measurement method used, separator design itself, layout, vibration phenomena, among others). In fact, the only potentially valid explanations were: a significant water entrainment in the recycled steam, a too small particle size of the liquid phase to be centrifuged or else a strongly heterogeneous distribution of the water flowrate among the 4 or 5 cells that make up the separator.

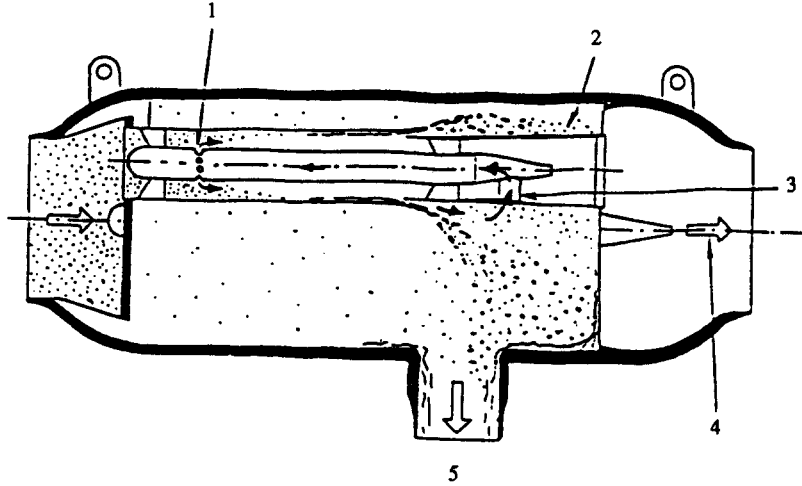
The first explanation (significant water entrainment in the recirculation steam) was found to be sound by performing tests on some separators to check the impact of a change in the way the recycled steam is reinjected. Figure 4 shows the initial injection mode, called downstream recirculation, as well as the new mode, called upstream recirculation. A number of separators were thus retrofitted, including all the separators not yet installed. However, it appeared, during subsequent on-site performance controls, that the alteration introduced did not result, for all applications, in an improvement as high as that observed on the test rig (note that, this time again, the test rig, because of its limited capabilities, was not adapted to the testing of all the separation applications). In one case even (HVS handling the highest flowrates) the change did not improve the separator performance at all.

It is as yet technically very difficult, if not impossible, due to the lack of measuring means, to establish the validity of the other explanations mentioned above (particle size, heterogeneity of the liquid phase distribution).

Finally, after these test campaigns and theoretical studies, it was impossible to clearly account for the lower separation efficiency recorded on site. However, a large data base was compiled from the numerous tests carried out. Table 1 contains some of the data entered into the data base. The test results can be classified by using a dimensionless number characterizing the liquid phase

Principle of the downstream recirculation HVS

- 1 Reinjection holes
- 2 Dense mist
- 3 Piece in the shape of a water droplet
- 4 Dry steam
- 5 Separated water



Principle of the upstream recirculation HVS

- 6 Upstream water droplet shaped piece
- 7 Separation lip
- 8 Collected water tank
- 9 Separation cell
- 10 Wet steam

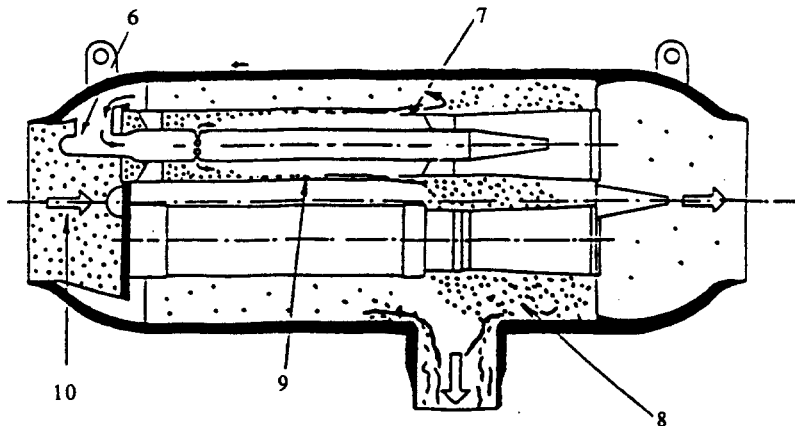


Figure 4. Downstream and upstream recirculation HVSs.

entrained by the gaseous phase in the film on the wall. This dimensionless number is directly derived from a number defined by Ishii & Grolmes (1975) by substituting the dynamic viscosity of the gaseous phase for that of the liquid phase in the original expression. This dimensionless number is therefore written

$$N_{Re} = \frac{\mu_G V_G}{\sigma} \sqrt{\frac{\rho_G}{\rho_L}}$$

where μ denotes the dynamic viscosity, σ is the interfacial tension, V is the velocity and ρ is the density, while the subscripts G and L correspond to the gaseous and liquid phases, respectively.

Table 1. Operating characteristics of HP recirculation-type HVS (the values given correspond to the rated operating conditions)

	Operating pressure (MPa) at the inlet	Steam wetness upstream of the separator (%)	Gas velocity in the reference section V_G (m/s)
CP2 type 900 MW PWR units			
Extraction line No. 5	2.15	7.5	50
P4 type 1300 MW PWR units			
Extraction line No. 6	2.70	10.1	45
Extraction line No. 5	1.70	16.8	50
P'4 type 1300 MW PWR units			
Extraction line No. 6	2.70	0.2	30
Extraction line No. 5	1.60	13.8	65

Figure 5 shows the test results obtained on site using this modified number $E_s = f(N_{Re})$ (where E_s is the separation efficiency). This number was successfully used for the subsequent design of the recirculation HVSs:† there is indeed a critical value of the entrainment number below which the separation efficiency remains quite satisfactory.

3. FEASIBILITY OF A TEST ON AN ANALOGUE FLUID SYSTEM

Additional tests on a steam/water system being useless due to the lack of adequate measuring means, EDF decided to perform a test on an analogue system to better understand the phenomenon resulting in the lower separator efficiency. Several choices had to be made: the modelled separator type, the similarity criteria, the analogue fluid system and the test loop to be used for the study.

3.1. Choice of the modelled separator

Separators with an operating pressure of some 2 MPa were chosen because the pressures used in the initial application ranged from 1.6 to 2.8 MPa. This choice is justified, first, by the large number of separators working under these conditions and, second, by the multiple test results available.

Moreover, it was decided that the so-called upstream recirculation HVS, considered to be the final version of recirculation HVSs, would be modelled. A separator on an extraction line in a 900 MW unit of the CP2 series was chosen as the reference case. This unit is supposed to be operating at its rated (full power) power. The values of the various physical quantities are given in table 2.

3.2. Choice of the similarity criteria

3.2.1. *Simplifying assumptions.* The physical phenomena involved in the operation of an HVS of the HP recirculation type are many. Therefore, to facilitate the definition of a test on an analogue fluid system, a number of simplifying assumptions must be used. These assumptions are as follows:

- There is no strong interaction between the droplets and the gas: this assumption is used for calculating the separator efficiency.
- The effect of the recycled gas reinjection on the gas flow in the centrifugation area‡ can be neglected; this assumption is also used for the calculation of the separator efficiency.
- The gas flow is little slowed down in the centrifugation area‡ (or, in other words, frictional pressure drops are negligible in this area).
- When the Reynolds number is large enough, a moderate deviation of its value as against that in the real unit does not modify the influence of the turbulence of the gas flow in the centrifugation area.‡

†Thus, a separation efficiency of approx. 97.5% was measured on the HVSs installed in the Loviisa power plant (Finland) to dry the extracted HP steam (pressure = 1.7 MPa) (Dueymes 1989c).

‡This is the area lying between the rotating vanes upstream and the separation lips downstream.

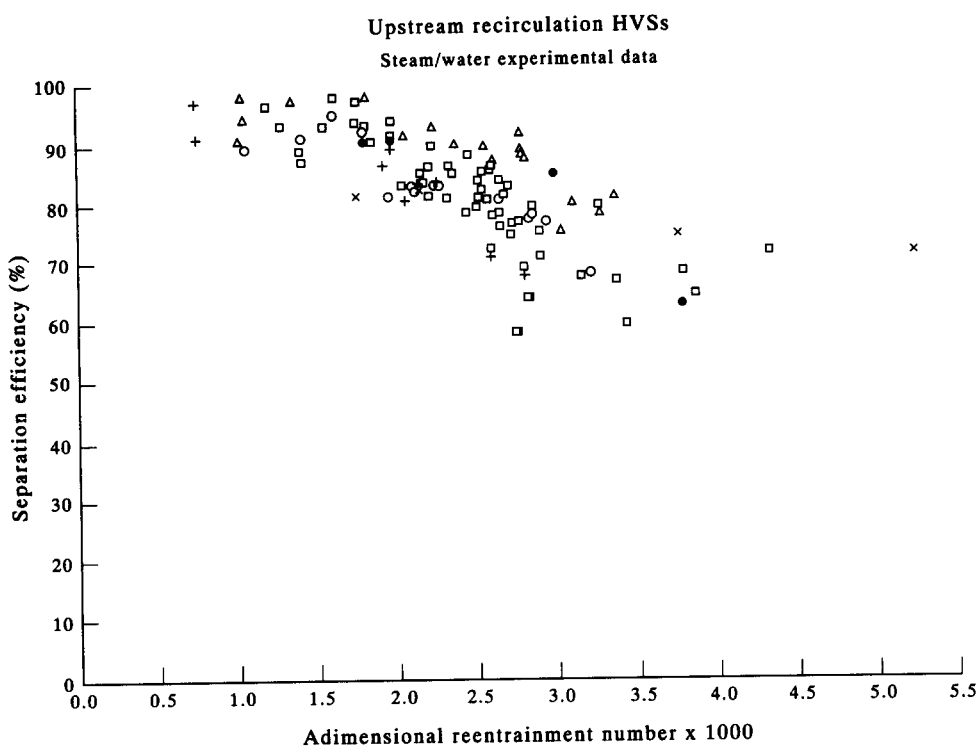


Figure 5. Steam/water experimental data (on-site measurements).

These four assumptions are used for calculating the trajectories of liquid particles. If the first three assumptions do not seem very restrictive, the fourth must be used with great caution.

3.2.2. Final selection of similarity criteria. An HVS cell is made of four areas—these are following the direction of the flow (see figure 4):

- *Area 1—cell inlet*

This is a cylinder in which the flow is a two-phase gas/liquid flow. In normal HVS operating conditions, this flow is an annular-dispersed flow (Delhaye *et al.* 1981); the water flows in rivulets or in a film at the wall and as droplets entrained by the gas.

- *Area 2—fixed turning vanes*

The flow is of the same type as at the cell inlet but a substantial fraction of the liquid droplets will impinge upon the turning vanes.

Table 2. Values of the physical quantities characterizing the real operating conditions to be simulated

$p = 2.15 \text{ MPa}$
$t = 216.1^\circ\text{C}$
$\rho_G = 10.78 \text{ kg/m}^3$
$\rho_L = 845.3 \text{ kg/m}^3$
$\sigma = 34 \cdot 10^{-3} \text{ N/m}$
$\mu_G = 16.3 \cdot 10^{-6} \text{ kg/m/s}$
$\mu_L = 125.5 \cdot 10^{-6} \text{ kg/m/s}$
$W_G = 11.4 \text{ kg/s}$
$W_L = 0.79 \text{ kg/s}$
$x = 0.935$
$D = 0.1643 \text{ m}$
$D_h = 0.076 \text{ m}$
$V_G = 50 \text{ m/s}$

- *Area 3—centrifugation area*

The droplets (in particular those formed by the water films torn away from the vanes) will be centrifuged. Most of the droplets will reach the cell shell and coalesce into a liquid film.

- *Area 4—cell outlet*

This is the area downstream from the separation lips. In this area the flow is practically single-phase.

To carry out a study on an analogue fluid system, the preponderant characters of each area must first be identified. Area 4 raises no specific problem since the flow is nearly single-phase. In areas 1 and 2, although the flow is two-phase, the gas flow seems more important to simulate: indeed, the void fraction of this flow is known to be very close to 1. Furthermore, we know that, with a constant gas flowrate, the liquid flowrate can be varied over a wide range without affecting the annular-dispersed nature of the flow. Finally, in area 3, two physical phenomena must absolutely be kept identical: the centrifugation mechanisms, on the one hand, and the quasi-stratified nature of the flow, on the other (flow of a film on the wall around a virtually single-phase gas flow).

Therefore, it appears that to study the operation of an HVS on an analogue, the following requirements must be met:

- Similarity of the gas flow upstream of the centrifugation area. Some freedom is left regarding the liquid phase as long as the annular-dispersed character of the gas/liquid flow is preserved.
- Similarity of the centrifugation mechanisms.
- Similarity of the liquid film flow in the centrifugation area.

The corresponding dimensionless numbers that will have to be taken into account are:

- *A Reynolds number for the gas flow, i.e. $Re_G = \rho_G V_G D / \mu_G$*

Or, should it be impossible to satisfy the Re_G number in the mockup, a “partial similarity” could nevertheless be achieved by keeping the Euler number Eu_G of the gas flow instead of the Re_G number (this “partial similarity” would only be valid if the gas flow remained fully turbulent). The Euler number Eu_G is written

$$Eu_G = p / (\rho_G \cdot V_G^2).$$

We can note that the selection of the gaseous Euler number (obtained from the dynamic head) as a scaling criterion was also made by Mauro *et al.* (1990) in another study involving steam/water separators.

- *The gas/liquid density ratio, ρ_G / ρ_L*

This ratio plays a major part in the simplified equation describing the drop movement. [On the role played by the number ρ_G / ρ_L in studies on separators, refer, for example, to Millington & Thew (1983), Boivin *et al.* (1987) or Mayinger (1976).]

- *A Weber number for the liquid film flow, i.e. We_f*

The definition given by Ishii & Grolmes (1975) or Van Rossum (1959) can be used, i.e.

$$We_f = \rho_G V_G^2 \delta / \sigma,$$

where δ denotes the liquid film thickness. We can also write a similar relation but with the liquid mass flowrate W_L instead of the thickness δ . Assuming that δ^2 is negligible compared to D^2 and that V_L is directly proportional to V_G for a given water flowrate,† we can write the following dimensionless number:

$$We_f = \rho_G V_G W_L / (\rho_L \sigma D).$$

These two expressions (incorporating either δ or W_L) will be used later on.

†The tests performed show that this is a realistic assumption over a relatively broad working range.

3.3. Choice of the fluid system

As regards the liquid phase, it seemed convenient to use water for a mockup test. As concerns the gaseous phase, argon was selected due to its physical and chemical characteristics. At a pressure of 775 kPa and a temperature of 20°C, the water/argon system exhibits the same density ratio as the water/steam system at 2.15 MPa and 216°C.

3.4. Choice of the test loop for the study

At Chatou EDF has a two-phase water/Freon R13B1 test loop called M.E.D.O.C. (Moyens d'Essais Diphasiques pour l'Obtention de Corrélations). This loop is described by Boivin *et al.* (1987). A brief study showed that a water/argon HVS cell could be tested on this test facility without requiring major changes in the loop.

4. DEFINITION OF THE MOCKUP GEOMETRY

Due to the capacity of the gas compressor, it quickly became evident that the mockup scale should not exceed 0.5. The scale finally chosen is 0.45 because of the size of standard tubes.

A brief study showed that Re_G cannot be kept within the 0.45-scale mockup. Were it to be kept within the mockup, gas velocities through the straightening vanes would be very high (> 200 m/s) leading to unrepresentative compressibility effects. On the contrary, **keeping Eu_G on the 0.45-scale mockup is possible** when considering the gas compressor capacity as well as the fully-turbulent nature of the gas flow. Similarly, keeping We_L on the 0.45-scale mockup is possible too. In fact, we can verify that, when the reference case described in table 2 is simulated, the two-phase flow in the mockup is still of the annular-dispersed type, i.e. the same as in the real unit (since the mass quality of the flow in the mockup x^M is 0.52†). However, simultaneously satisfying Eu_G and We_L is not without consequences if we consider the flow of the liquid film through the annular skimmer slot. In fact, we estimated, by roughly evaluating the film thickness from results presented by Fukano & Ousaka (1989), that the relative thickness of the liquid film in the mockup (δ^M/D^M) would be more than 10 times greater than in the real unit (δ/D); where δ is the mean thickness of the liquid film in the centrifugation area and D is the diameter of the HVS cell shell.

We deduced that experimental results on the mockup could be compared with experimental results on the real unit only in cases where the thickness of the liquid film is reasonably smaller than the width of the annular skimmer slot (in the mockup), in order to avoid obstruction phenomena. In other words, tests of the mockup with $We_L \geq 140$ will not correctly reproduce steam/water tests.

4.1. Summary

This brief study shows that if the dimensionless numbers ρ_G/ρ_L , Eu_G and We_L (or We_r) are kept, we can correctly simulate, under a wide range of running conditions, the operation of an actual HVS cell fed with wet steam at a pressure of 2.15 MPa on a 0.45-scale model supplied with water/argon at a pressure of 775 kPa.

Thus table 3, containing all the physical quantities and dimensionless numbers corresponding to the real fluid system as well as to the analogue fluid system, can be compiled for the reference case.

Figure 6 shows the water/argon mockup.

5. TESTS OF THE WATER/ARGON MOCKUP

5.1. Preliminary studies

Before performing the tests strictly speaking, theoretical studies were conducted to assess the impact of the scale reduction on the behaviour of the HVS cell.

†The superscript M concerns the mockup study. It will be used in the following sections.

Table 3. Values of the physical quantities and of the dimensionless parameters for a full-scale unit operating with a water/steam system and for 0.45-scale mockup operating with water/argon (similarity criteria: Eu_G and We_L . Application: extraction line No. 5 of the 900 MW CP2 power plant series)

Dimensionless parameter or physical quantity	Operation with water/steam (geometrical scale: 1)	Operation with water/argon (geometrical scale: 0.45)
Pressure (MPa)	2.15	0.775
Temperature ($^{\circ}C$)	216.1	20
ρ_G (kg/m ³)	10.78	12.78
ρ_L (kg/m ³)	845.3	998.6
σ (N/m)	$34.0 \cdot 10^{-3}$	$72.8 \cdot 10^{-3}$
μ_G (kg/m/s)	$16.3 \cdot 10^{-6}$	$22.4 \cdot 10^{-6}$
μ_L (kg/m/s)	$125.5 \cdot 10^{-6}$	$1002.6 \cdot 10^{-6}$
ρ_G/ρ_L	0.0128	0.0128
V_G : gas velocity in the reference section (m/s)	50	27.6
Re_G (Reynolds number of the gas)	$5.4 \cdot 10^6$	$1.2 \cdot 10^6$
Eu_G (Euler number of the gas)	79.8	79.8
N_{Re} (re-entrainment number for upstream of the cell)	$2.71 \cdot 10^{-3}$	$0.96 \cdot 10^{-3}$
Gas mass flowrate, W_G (kg/s)	11.4	1.517
Water mass flowrate, W_L (kg/s)	0.79	1.376
Mass quality of the flow, $x = W_G/(W_G + W_L)$	0.935	0.524
Lockhart–Martinelli parameter, X	0.0126	0.152
Superficial velocity of water in the centrifugation area, j_L	0.056	0.406
Re_L (Reynolds number of the liquid)	$6.2 \cdot 10^4$	$3.0 \cdot 10^4$
Eu_L (Euler number of the liquid)	$1.6 \cdot 10^6$	$9.4 \cdot 10^3$
Fr_L (Froude number of the liquid)	$1.95 \cdot 10^3$	$227 \cdot 10^3$
We_L (Weber number of the liquid)	90.2	90.2
Separation efficiency of the cell, E_S (%)	Measured value: 89	Measured value: 91

The first study concerns the recirculation rate in the separator, i.e. the percentage of the recycled gas flowrate (assumed to be dry) in the total incoming gas flowrate. This study shows that the scale reduction has no impact.

The second study concerns the separation efficiency: clearly, the scale reduction results in increasingly small particles being trapped, when Re_G is the same in the mockup and in the real unit.

Since the mechanisms of the liquid particle centrifugation and of the liquid film transport in the centrifugation zone clearly appear as essential parameters of the separation efficiency, they should be reproduced in a scale model as closely as possible. When Eu_G is kept constant, the calculated separation efficiencies of the real separator and of the mockup are perfectly comparable (for the same drop size).

5.2. Description of the test facility

The test facility is shown in figure 7. The main components of the circuit are:

- The argon compressor (4). This is a non-lubricated piston compressor with a compression ratio of approx. 1.35.
- The argon flowmeters (5): two flowmeters with different measuring ranges are used; they are turbine flowmeters.
- The separating tank (2). This large-capacity tank (5 m³) is designed to eliminate the residual moisture at the test chamber outlet.
- The water tank (8). This tank is used both to collect the water separated in the test chamber and to inject water into the argon circuit. To be sure that the separated water flows purely by gravity this tank is provided with a pressure equalizing pipe connected to the test chamber.
- Water flowmeters (6) and (10). These two electromagnetic flowmeters are used to meter the separated and injected water flowrates, respectively.
- An injection pump (9). This injects water into the argon circuit.
- A Plexiglas section (7). This is used to make sure that the separated water flows without entraining gases.
- Auxiliary circuits (3) and (12). These are mainly used to add argon and water into the test loop.

Annular skimmer slot

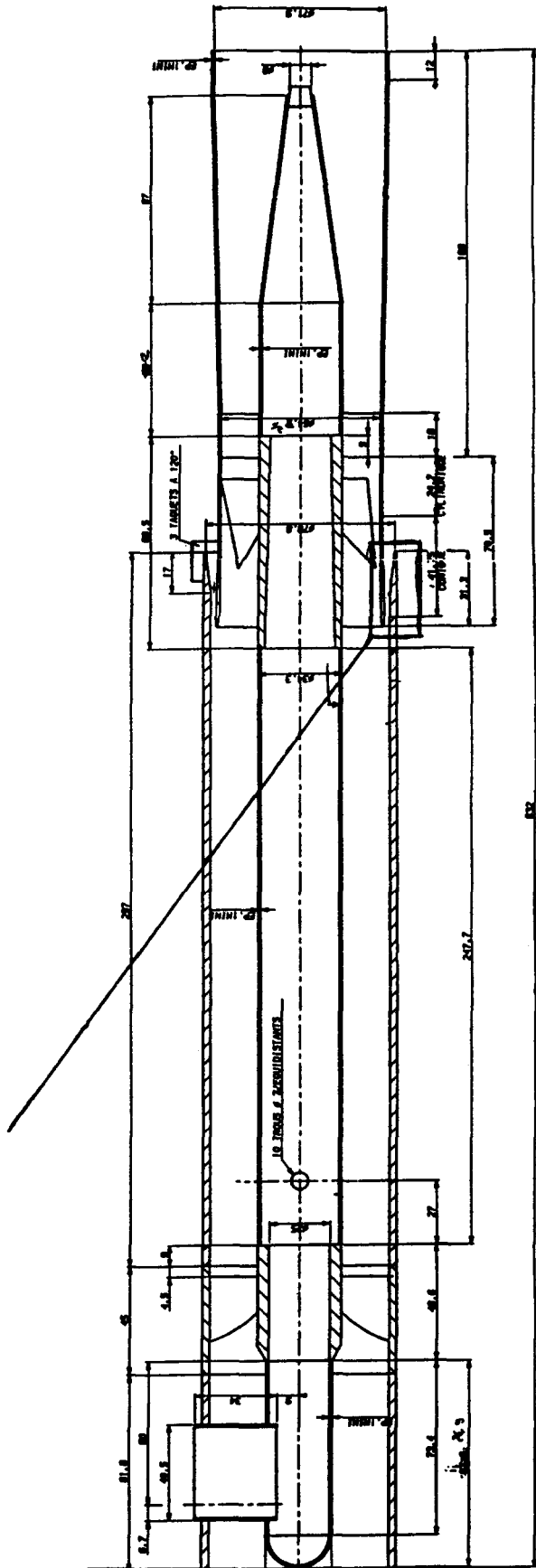


Figure 6. HVS cell tested on the MEDOC loop.

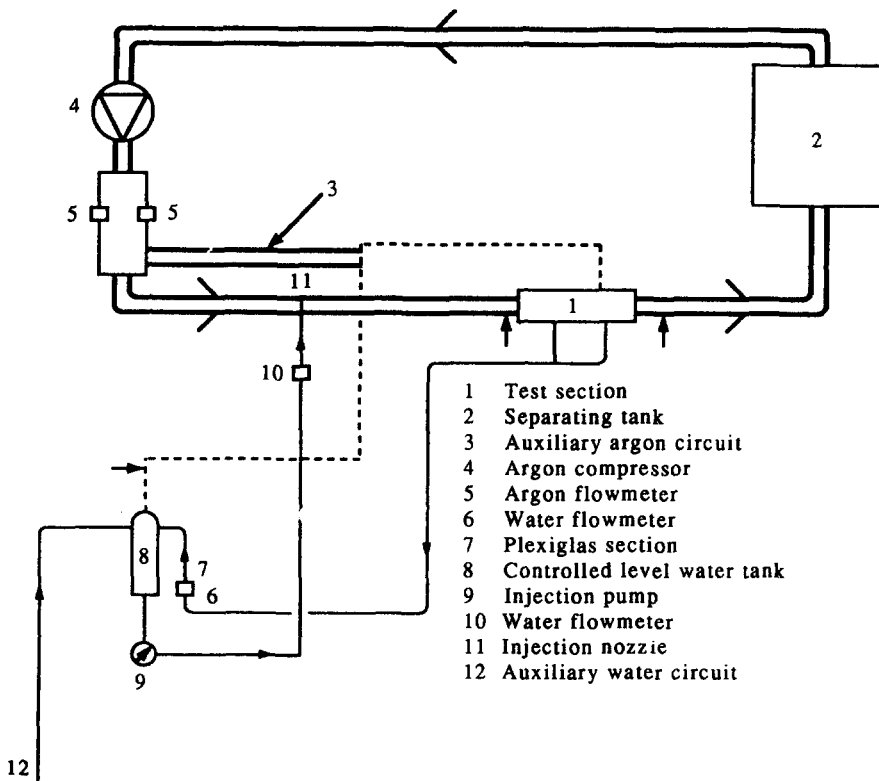


Figure 7. Description of the test facility.

- An injection device (11). This consists of a FULLJET injection nozzle mounted inside the pipe, and the water is injected in the same direction as the gas stream.
- Finally, the test chamber strictly speaking (1).

The test chamber consists of a watertight parallelepiped with the following internal dimensions: $1100 \times 137 \times 180$ mm. The HVS cell is located at the centre of the test chamber. Four Plexiglas half-cylinders are stuck onto the lateral walls of the chamber; they are used to simulate the presence of neighbouring HVS cells, since real units comprise several cells. The inner size of the chamber, once fitted with all its instrumentation, is chosen so that the mean velocity of the recycled gas roughly corresponds to the gas velocity in a real unit (i.e. some 1.2 m/s under normal operating conditions). The precise location of the HVS cell in the test chamber is shown in figures 8 and 9.

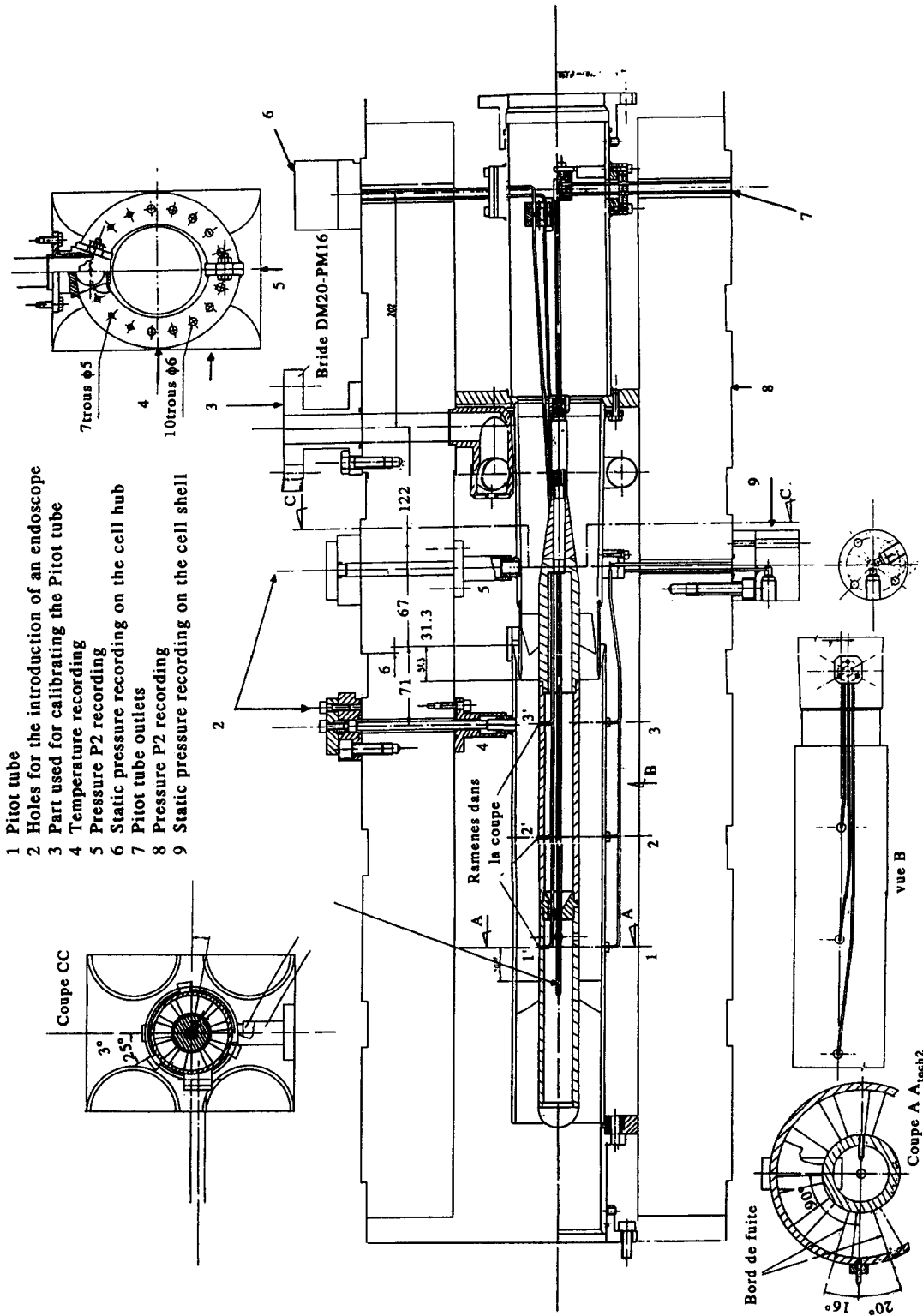
5.3. Measuring means

The water and argon flowrates are measured with the flowmeters described above (relative accuracy: approx. 1%).

The recycled gas flowrate is measured with a Pitot tube placed inside the hub of the HVS cell; this Pitot tube is calibrated once positioned. The accuracy of the flowrate measurement amounts to approx. 10%, considering that the water entrainment by the recycled gas cannot be taken into account. In addition to the flowrate, the pressure (at the argon flowmeter level in the test chamber, at several points on the shell and hub of the HVS cell and at both ends of the test chamber) and the temperature (at the argon flowmeter level and in the test chamber) are measured.

The recorded values are automatically processed. A computer determines all the quantities in real time based on the sensor characteristics, the physical properties tables of argon and water as well as the calibration curves of the Pitot tube.

After various tests, we found out that a series of 10 acquisition cycles separated by a 10 s time interval provided a fair compromise between acquisition numbers, acquisition times and accuracy.



- 1 Pitot tube
- 2 Holes for the introduction of an endoscope
- 3 Part used for calibrating the Pitot tube
- 4 Temperature recording
- 5 Pressure P2 recording
- 6 Static pressure recording on the cell hub
- 7 Pitot tube outlets
- 8 Pressure P2 recording
- 9 Static pressure recording on the cell shell

Figure 8. Internal instrumentation.

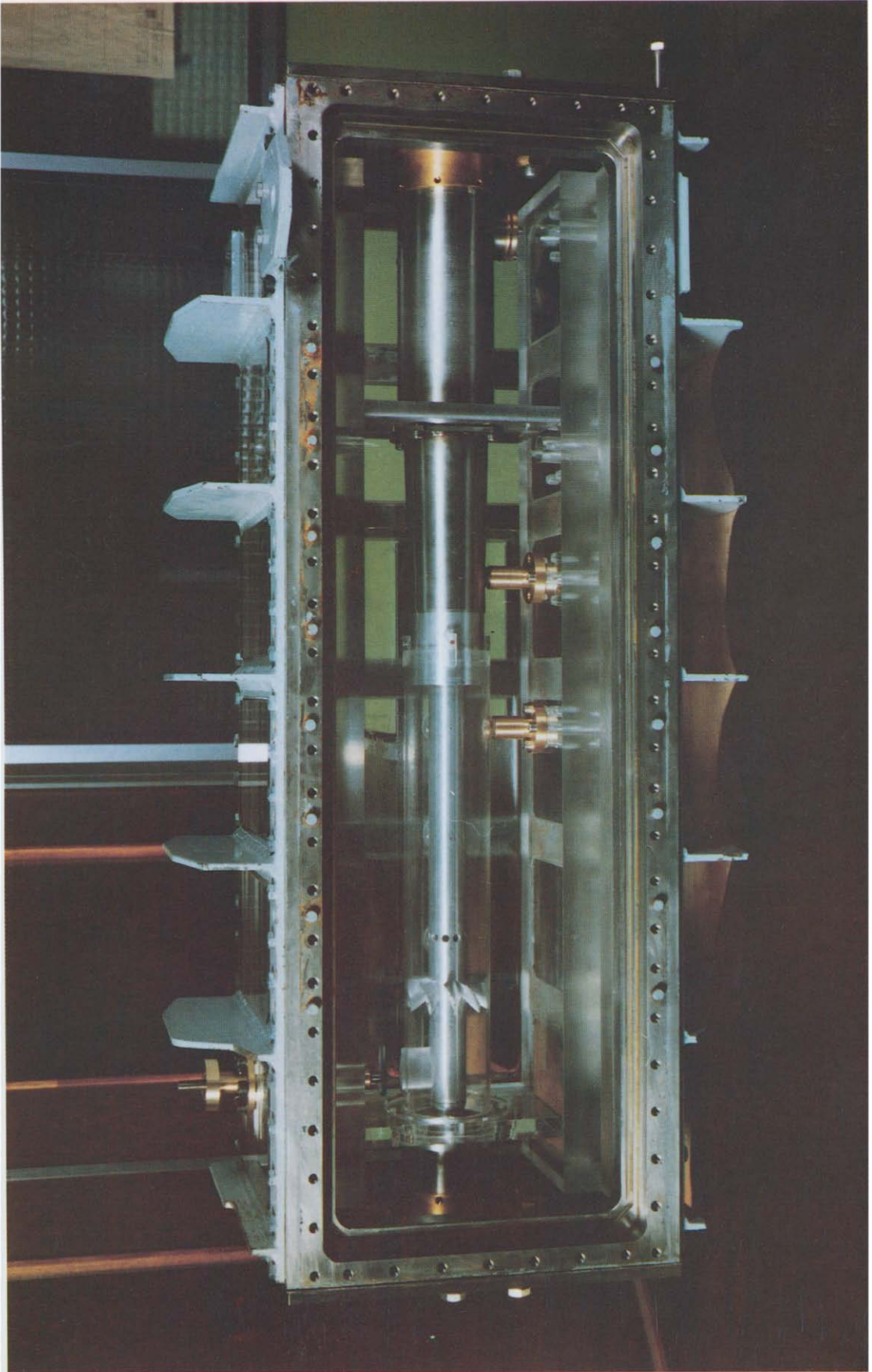


Figure 9. The test chamber.

Note, finally, that an endoscope can be introduced in two places: immediately upstream of the separation lips and downstream from the flow-straightening vanes.

6. TESTS PERFORMED

6.1. Preliminary remarks

Only the measures of water flowrate and separation efficiency will be presented in detail. The other test results can be summarized as follows:

- Pressure drop in the mockup. The pressure drop coefficient for the mockup is about the same as for the actual separator, although slightly higher. This difference is partly due to imperfections in the construction and assembly of the vanes, resulting in secondary losses larger in the small-scale separator than in the full-scale one. Nevertheless, a slight increase in the pressure drop coefficient is to be expected since the Reynolds number of the gas flow is smaller than in the real unit.
- The gas recirculation rate in the mockup. This is the ratio of the recycled gas flowrate to the incoming gas flowrate and corresponds to the anticipated values; it amounts to 4–5%.
- The amount of water entrained by the recycled gas. This is very low in most cases tested (except for the operating conditions where very high gas flowrates have to be processed).

6.2 Water injection

The mockup behaviour (pressure drop or separation efficiency) is in no way affected by the water injection mode (type of nozzle used, use or not of an injection nozzle). This is probably due to the water being injected relatively far upstream of the test chamber (at a distance more than 30 times the pipe diameter): indeed, due to its full turbulence, the flow reaches hydrodynamic equilibrium before the test chamber.

Finally, most of the operating conditions tested have been obtained without having to use an injection nozzle so that as large a range of water flowrates as possible could be examined.

6.3. Variation range of the various parameters

Water flowrate to be processed in the mockup: from 0 to 2.07 kg/s.

Argon flowrate to be processed in the mockup: from 0 to 4.45 kg/s.

Static pressure in the test chamber: from 590 to 965 kPa.

7. ARGON/WATER RESULTS

All the separation efficiency measurement results can be presented as in figures 10 and 11. These figures represent the variation of the separation efficiency as a function of the dimensionless number Eu_G^M defined previously; the parameter used is We_L^M . The separation efficiency of the HVS cell is globally optimal for We_L^M ranging from 50 to 250; in this range, the separation efficiency is satisfactory (i.e. above some 90%) when Eu_G^M remains between 20 and 150. The efficiency drops when We_L^M is low (< 10). At the same time as the efficiency deteriorates, the dispersion of the results is very important (especially when $We_L^M < 5$). When the separator operates with very low water flowrates, a continuous water film cannot form in the centrifugation area. Water then flows in thin rivulets which grow increasingly unstable (radially and tangentially) as they draw nearer to the annular skimmer slot and cannot be properly removed.

8. COMPARISON OF ARGON/WATER AND STEAM/WATER RESULTS

The results for the full-scale water/steam tests and the 0.45-scale water/argon tests can be directly compared in figures 12–14. As can be seen, there is a good agreement between the two series of

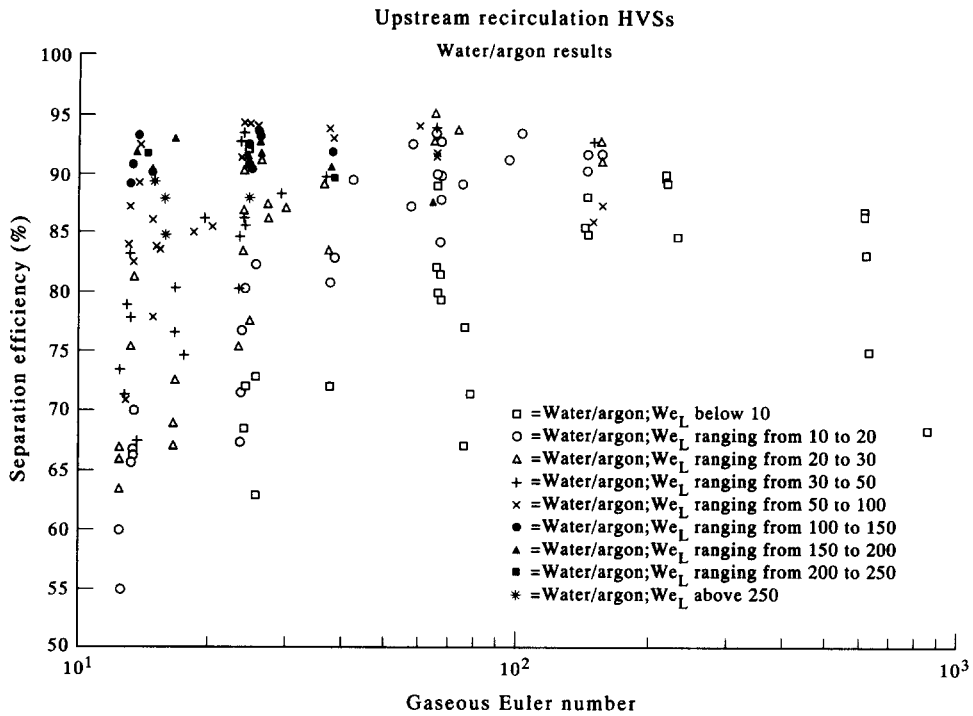


Figure 10. Water/argon results; influence of We_L .

tests. The compared range for the parameter We_L is 10–140. There is no data for a steam/water operation with $We_L < 10$; when $We_L > 140$, the efficiency recorded with water/argon is systematically better than with water/steam. This difference is normal since we know that such values of We_L are not within the validity range possible for the analogue fluid system.

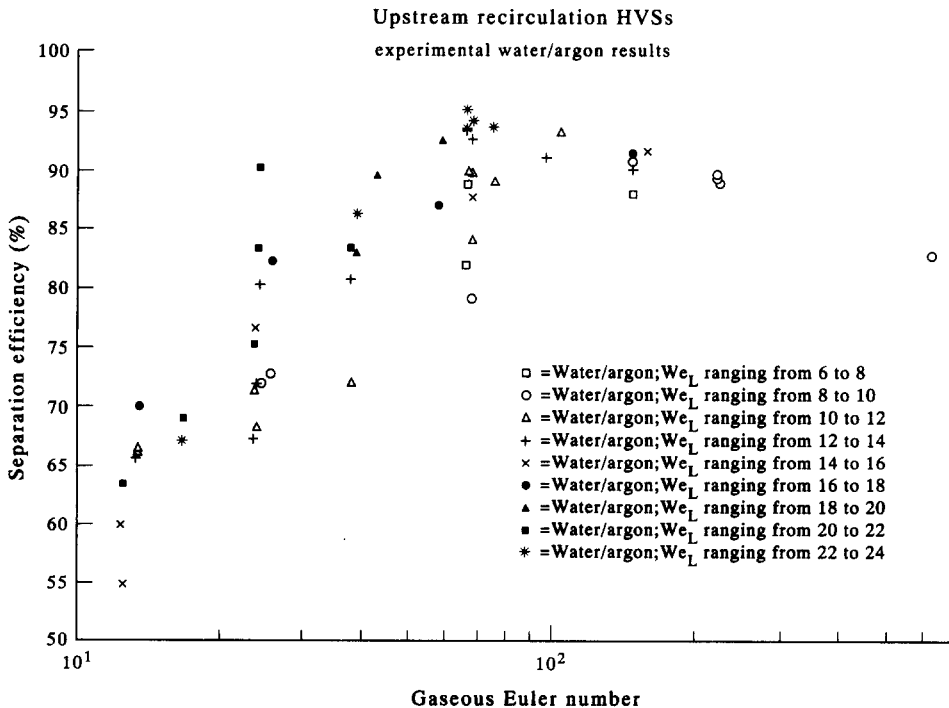


Figure 11. Water/argon results; We_L ranging from 6 to 24.

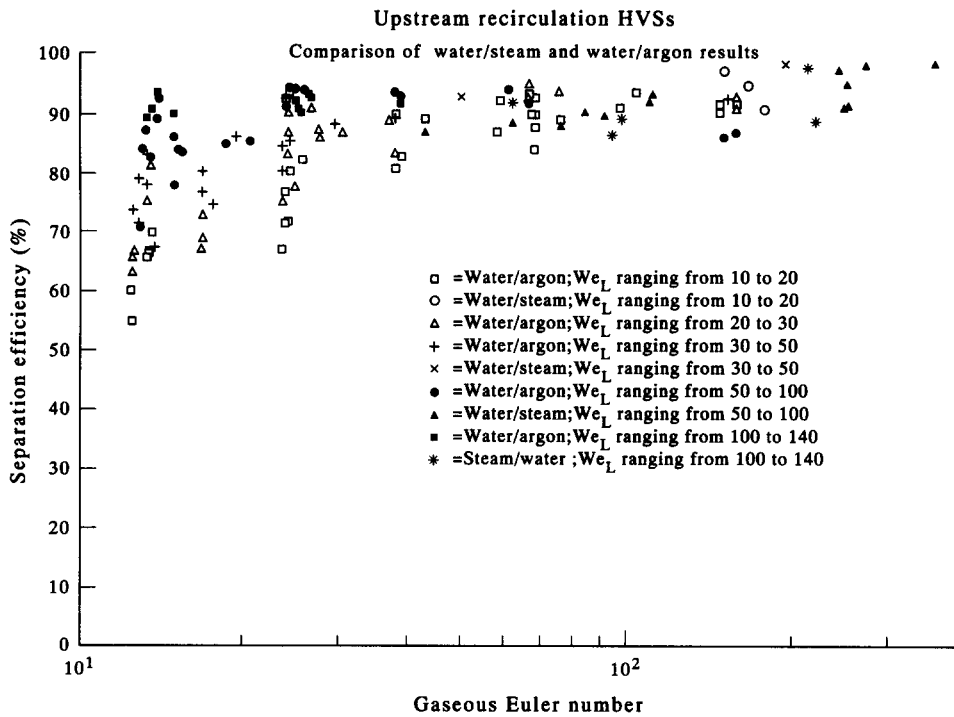


Figure 12. Comparison of water/argon and steam/water operations.

9. CONCLUSIONS

The operation of a centrifugal separator (HVS) was studied with a 0.45-scale mockup on a test loop of the Direction des Etudes et Recherches at EDF. In the framework of this study, the actual fluid system (water/steam in thermodynamic equilibrium at a pressure of some 2 MPa) was replaced by a water/argon system at a pressure of about 740 kPa and at a temperature of 25°C.

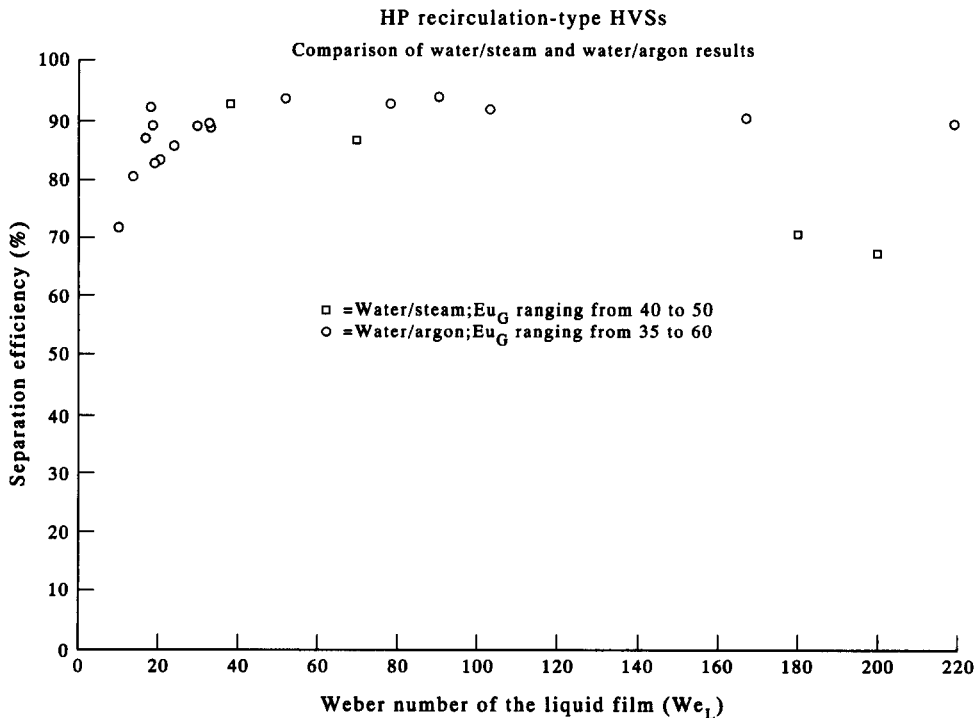


Figure 13. Separation efficiency vs We_L ; Eu_G ranging from 35 to 60.

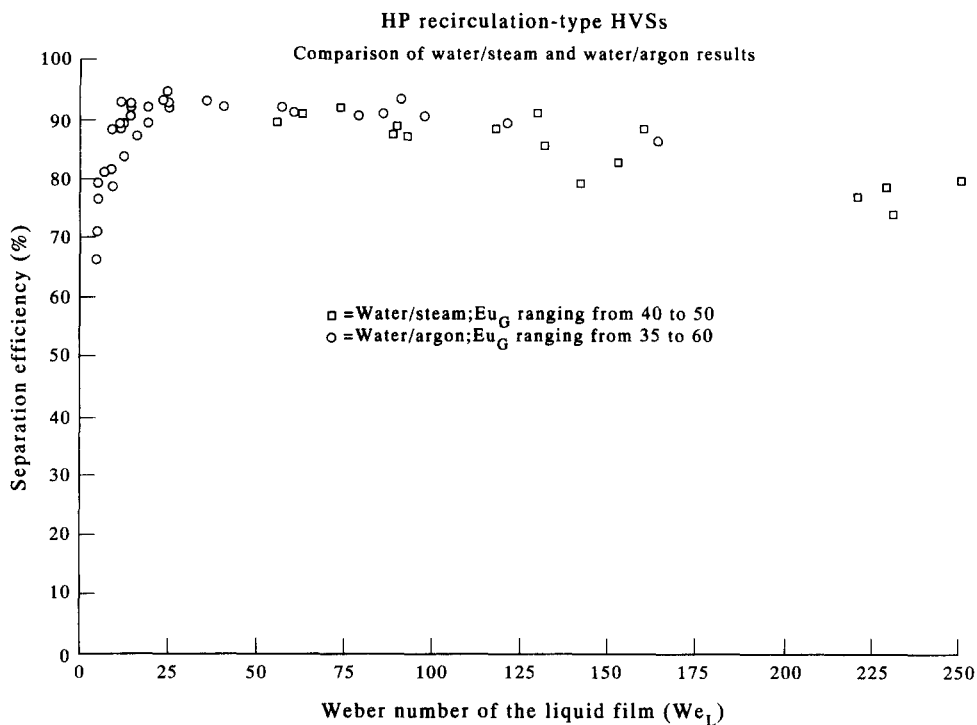


Figure 14. Separation efficiency vs We_L ; Eu_G ranging from 60 to 110.

Similarity criteria have been defined: the maintenance of the flow patterns; a Euler number Eu_G for the gas flow—which is kept to reproduce the centrifugation mechanisms as well as the incoming gas flow; a Weber number describing the liquid film flow in the centrifugation area We_L (or We_r) and the density ratio of the two phases ρ_G/ρ_L . Note that the first two criteria (maintenance of the flow patterns and Eu_G) were also used by Mauro *et al.* (1990) in a study of another type of steam/water separators.

As concerns the behaviour of the HVSS (in terms of their separation efficiency), we can now get a reliable evaluation of their efficiency by using two dimensionless numbers: We_L and Eu_G .

The performance deterioration which was observed in some industrial sites is ascribed to the liquid film flow in the centrifugation area.

Acknowledgements—The author wishes to thank B. Danevcic, P. Décembre, A. R. Laali, A. Libéreau and G. Piérotti (EDF, R&D Division), for their participation in the test program, and M. Y. Lecoffre (Scientific Consultant) for his contribution to the final analysis.

REFERENCES

- BOIVIN, J. Y., BUSSY, B. & PIEROTTI, G. 1987 PWR steam generators: a set of experimental programs for three-dimensional code validation. Paper presented at the *ASME Winter A. Mtg*, Boston, MA, Paper 87-WA/NE-4.
- CERDAN, J. P. & TALLEU, P. 1984 The high velocity separators. In *Multi-phase Flow and Heat Transfer III. Part A: Fundamentals*, pp. 445–465. Elsevier, Amsterdam.
- DELHAYE, J. M., GIOT, M. & RIETHMULLER, M. L. 1981 *Thermohydraulics of Two-phase Systems for Industrial Design and Engineering*. Hemisphere/McGraw-Hill, New York.
- DUEYMES, E. 1989a Wet steam flows in large-diameter pipes: flowrate, moisture and pressure drop measurements. *Int. J. Multiphase Flow* **15**, 901–909.
- DUEYMES, E. 1989b On-site measurement of the moisture-separator efficiency. Paper presented at the *IXth Conf. on Steam Turbines of Large Output*, Karlovy Vary, Czechoslovakia.

- DUEYMES, E. 1989c Loviisa Power Plant, Unit 1, Turbine 2—checking of performances of the high velocity separators which equip the piping extraction line no. 2 of the high pressure body of the turbine. Internal EDF/DER Memorandum HP43/89.19.
- DUEYMES, E. & PEYRELONGUE, J. P. 1990 Recent developments in the 'high velocity separators' technique. Paper presented at the *CHISA'90 Congr.*, Prague, Czechoslovakia.
- FUKANO, T. & OUSAKA, A. 1989 Prediction of the circumferential distribution of film thickness in horizontal and near-horizontal gas-liquid annular flows. *Int. J. Multiphase Flow* **15**, 403–419.
- ISHII, M. & GROLMES, M. A. 1975 Inception criteria for droplet entrainment in two-phase cocurrent film flow. *AIChE Jl* **21**, 308–318.
- MAURO, G., SALA, M. & HETSRONI, G. 1990 Improved Italian moisture separators (IIMS). *Nucl. Engng Des.* **118**, 179–192.
- MAYINGER, F. 1976 Scaling and modelling laws in two-phase flow and boiling heat transfer. In *Two-phase Flows and Heat Transfer* (Istanbul, Turkey)—Conf. Proc., Vol. 1, pp. 129–161.
- MILLINGTON, B. C. & THEW, M. T. 1983 Preliminary investigations on a cyclone for steam-water separation. In *Proc. Int. Conf. on the Physical Modelling of Multi-phase Flow*, Coventry, U.K., Paper K3.
- VAN ROSSUM, J. J. 1959 Experimental investigation of horizontal liquid films. *Chem. Engng Sci.* **11**, 35.